Journal of Metals, Materials and Minerals, Vol. 27 No. 2 pp. 6-11, 2017

Development of WO_3 Nanostructure by Acid Treatment and Annealing

T. Sanasi[1], S. Pinitsoontorn[1,*] , M. Horprathum[2], P. Eiamchai[2], C. Chananonnawathorn[2], and W. Hinchreeranun[2]

[1]Integrated Nanotechnology Research Center, Department of Physics, Faculty of Science, Khon Kaen University, Khon Kaen, 40002, Thailand
[2]Optical Thin- Film Laboratory, National Electronics and Computer Technology Center, Pathumthani, 12120, Thailand

Abstract

Tungsten oxide (WO_3) nanostructure is an interesting material for many applications such as batteries, gas sensors, photocatalysts, display utilizing, and smart windows. In this work, we fabricated the WO_3 nanoplates by sputtering, acid treatment and annealing. Firstly, a tungsten film was deposited on a silicon or glass substrate by sputtering. The film was then immersed in nitric acid (HNO_3) at 80°C. The effect of the exposure time, and annealing temperature was investigated. After the acid treatment, the tungsten oxide hydrate or tungstile ($WO_3 \cdot H_2O$) with nanoplate structure was developed. The optical transmittance in the visible range was significantly improved compared to the continuous tungsten film. The size of the nanoplate was found to increase with increasing the immersion time. The tungsten oxide hydrate nanoplates transformed into WO_3 after annealing at ≥ 200°C. Increasing annealing temperature resulted in the decreasing size of the nanoplates. The shape of the nanoplates became more of the rectangular shape with annealing. The optical transmittance of the WO_3 film increased with the annealing temperature up to 400°C.

Keywords: Tungsten oxide; Nanoplates; Acid treatment; Annealing

Introduction

Tungsten oxide (WO_3) nanostructure is an interesting material for many applications such as batteries, gas sensors, photocatalysts, display utilizing, and smart windows[(1-3)]. In order to prepare WO_3 nanostructured thin films, several methods have been used, for instance, chemical vapor deposition[(4)], electron beam deposition [(5)], spray deposition[(6)], and sol-gel spin coating.

Another interesting but simple method for preparing the WO_3 nanostructure is by using acid treatment[(7-10)]. In this method a continuous tungsten film/sheet is immersed in an acid solution for developing the WO_3 nanostructure. In particular, the nanoplate morphology is preferential formed by using this method. The acid treatment method shows several advantages over the other techniques, for example, simple set-up, fast, ability for up-scaling. Generally, nitric acid (HNO_3) was selected in the process due to its potential for oxidizing W film. The W film did not directly transform into WO_3 by acid immersion process but the intermediate phase (tungsten oxide hydrate, $WO_3 \cdot H_2O$) was usually formed. The $WO_3 \cdot H_2O$ phase could be easily transformed into WO_3 nanoplates by heat treatment. Although the previous literatures have reported the synthesis of WO_3 by the acid treatment process and its application in various fields[(7-10)], the detailed study for the effect of acid immersion time and annealing temperature on the morphology of the nanoplates and the optical transmission properties has not been researched. Therefore, the objective of this research is to study such topics in more details.

Experimental methods

Thin tungsten films were deposited on Si wafer or glass substrates by using pulsed DC sputtering under Ar atmosphere at 5 mTorr and the power of 100 Watt for 10 min. After that, to obtain the hydrated tungsten oxide ($WO_3 \cdot H_2O$) nanoplates, the acid treatment process was carried out. The samples were immersed in 1.5

* Corresponding author E-mail: psupree@kku.ac.th

DOI: 10.14456/jmmm.2017.xx

M HNO_3 at 80°C with the various immersion time of 30, 60 and 90 min. As subsequently shown in the next section, the films immersed in the acid for 90 min showed the clear and smooth surface of the $WO_3 \cdot H_2O$ nanoplates. Thus, this sample was chosen for the annealing process at the temperature range of 100–500 °C at the fixed time of 1 h. The annealing process transformed the $WO_3 \cdot H_2O$ to the WO_3 nanostructured film by removing water molecules.

The plan view and cross-section morphology of the films was investigated by using the scanning electron microscope (Hitachi, S4700). The phase and crystalline structure of the films were analyzed by using the X-ray diffraction technique (Rigaku, TTRAX III). The optical transmittance of the $WO_3 \cdot H_2O$ and WO_3 films deposited on glass substrate was measured by using the spectrophotometer (Agilent Cary, 7000).

Results and Discussion

Figure 1 shows the cross-section SEM image of the tungsten film after the deposition on Si wafer. It can be seen that the film is continuous and uniform with very smooth surface over a large scale. The film thickness was estimated to be around 72 nm (the average value from the measurement directly in the SEM image of over 10 locations).

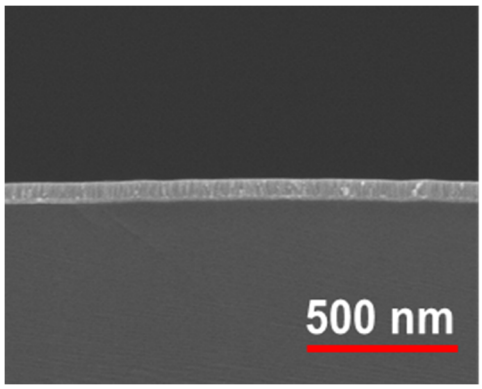

Figure 1. Cross section SEM image of the W film on Si wafer.

Figure 2 shows the plan view and cross section morphology of the films after the acid treatment. It is obvious that the film morphology has changed significantly compared to Figure 1. The HNO_3 acid has transformed the continuous W film into the nanoplate structure of the hydrated tungsten oxide ($WO_3 \cdot H_2O$). The nanoplated films also became thicker (> 400 nm). The thickness of the $WO_3 \cdot H_2O$ film as well as the average size of each nanoplate increased with the acid immersion time as summarized in Figure 3.

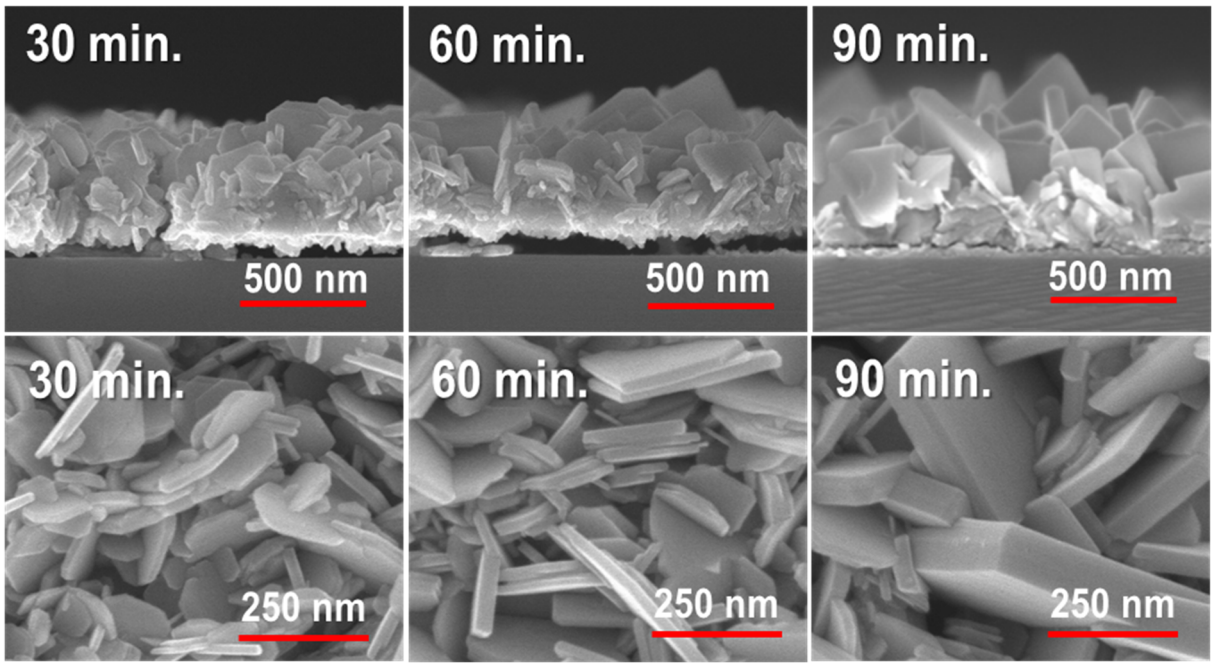

Figure 2. Plan view and cross section images of the $WO_3 \cdot H_2O$ nanoplated films after acid treatment of 30, 60 and 90 min.

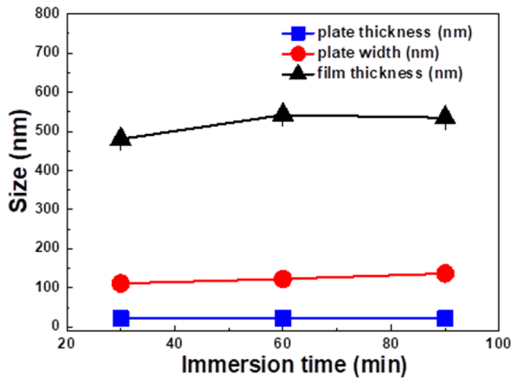

Fig 3. $WO_3 \cdot H_2O$ film thickness and the size of nanoplate as a function of immersion time.

The optical transmission spectra of the W film and the $WO_3 \cdot H_2O$ films are presented in Figure 4(a). There is a significant change in the spectra from the W film to the $WO_3 \cdot H_2O$ films. For the W film, the sample did not allow the light transmission throughout the measurement wavelength range, i.e. the film is mostly opaque for light from 200 to 2,000 nm. On the other hand, the $WO_3 \cdot H_2O$ nanostructured films show some transparencies in the visible and infrared spectra. The change in the optical properties can be explained from the formation of WO_3 in the samples after acid treatment. The introduction of oxygen to the W film change the metallic behavior of the W film into the insulating tungsten oxide films. This in turn also changed the electronic structure of the sample from no band gap (metallic) to wide band gap semiconductor, which did not absorb light in the visible range, and thus became more optically transparent. Figure 4(b) shows the average %transmittance in the visible range. The transmittance increased with acid immersion time. Again this could be explained from the reaction of oxygen with the W film. The longer the acid treatment, the more $WO_3 \cdot H_2O$ nanostructured film was formed.

The optical band gap of the sample as a function of acid immersion time was evaluated according to the equation.

$$(\alpha h\upsilon)^n = A(h\upsilon - E_g) \qquad (1)$$

where α , $h\upsilon$, A and E_g are absorption coefficient, photon energy, relation constant and optical band gap, respectively. By using n = 1/2 for indirect band gap semiconductors, and the extrapolation technique (Figure 5(a)), the optical band gaps as a function of acid immersion time are presented in Fig. 5(b). Obviously, one can see that the optical band gap increases with the longer immersion time as the oxidization of the W film is in a more advanced state.

Since the sample immersed for 90 min showed the clearest and smoothest morphology of the $WO_3 \cdot H_2O$ nanoplate, and the highest optical transmittance in the visible range, we have chosen this sample for the annealing treatment.

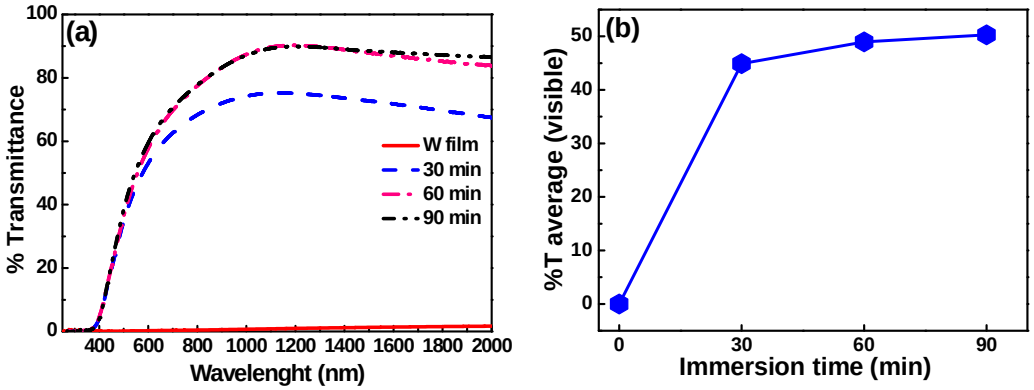

Figure 4. (a) Optical transmission spectra and (b) average transmittance of W film and $WO_3 \cdot H_2O$ films with different immersion time

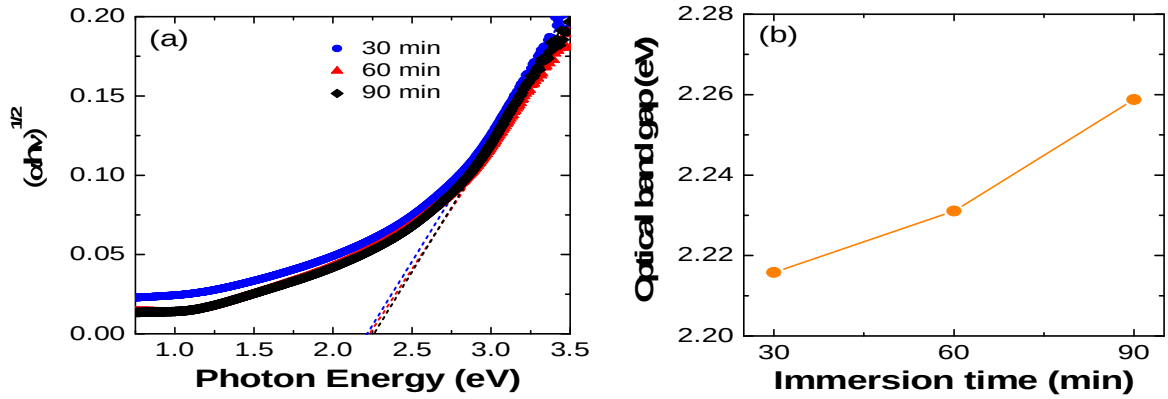

Figure 5. (a) Optical band gap estimation by extrapolation technique, and (b) optical band gap as a function of immersion time.

Figure 6 shows the plan view and cross images of the WO_3 nanostructured films after the heat treatment at 100–500°C. The annealing has no effect of the shape of the nanostructure, i.e. the nanoplate morphology was maintained up to 500°C. However, the thickness of the films was decreased and the width of individual nanoplates was slightly reduced as the annealing temperature increased (Figure 7) as a result of the removal of water molecules.

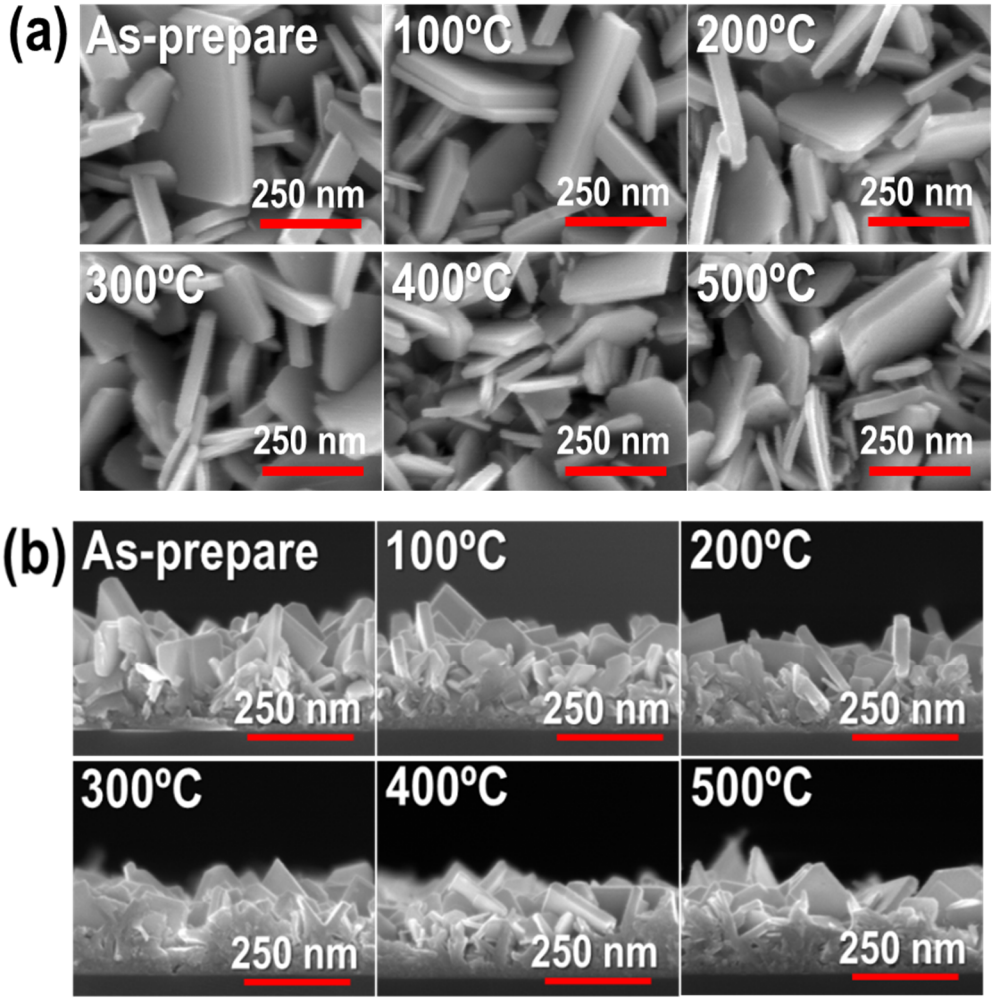

Figure 6. Plan view and cross section images of the W nanoplated films after 1 h annealing at 100–500°C.

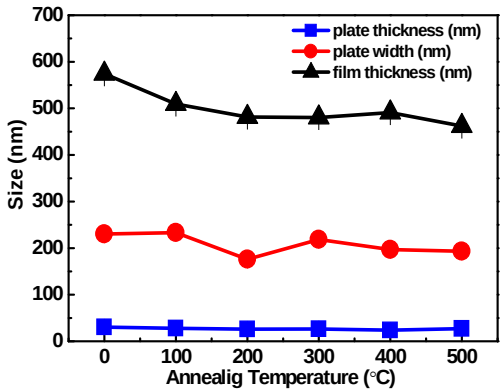

Figure 7. WO_3 film thickness and the size of nanoplate as a function annealing temperature.

The transformation of the $WO_3 \cdot H_2O$ to the WO_3 nanoplated films manifested in the optical transmission measurement. The transmission spectra of the non-annealed and the annealed WO_3 films in the wavelength of 200–2,000 are shown in Figure 8(a). The transmission curves look very similar for every sample. However, when plotted the average %transmittance in the visible range against the annealing temperature, a trend emerged as shown in Figure 8(b). The transmittance has a tendency to increase with annealing temperature. This is probably due to the removal of water molecules, making the more complete WO_3 films, and thus more optical transparent. The exception is for the sample annealed at 500°C where there is a sudden drop in the transmittance. The possible reasons for the sudden change could be from deteriorated and poorly deformed as the glass slide substrate melted. It should be noted that the transparency of all samples were still lower than 55% which could be probably due to a large surface roughness of the film.

The optical band gap of the samples as a function of annealing temperature could be was evaluated using the extrapolation technique according to the equation 1 as explained previously. The results are shown in Figure 9. The optical band gap has a tendency to increase with increasing annealing temperature up to 400°C due to the more complete formation of the WO_3 crystalline phase. At 500°C, a sudden drop in the band gap was found which was due to themelt of the glass slide substrate as discuss earlier.

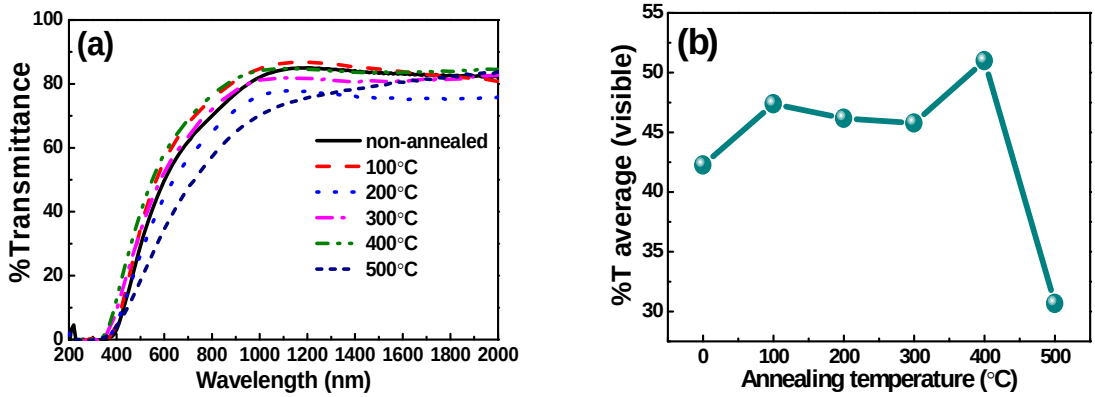

Figure 8. (a) Optical transmission spectra and (b) average transmittance of the $WO_3 \cdot H_2O$ film and WO_3 films with different annealing temperature.

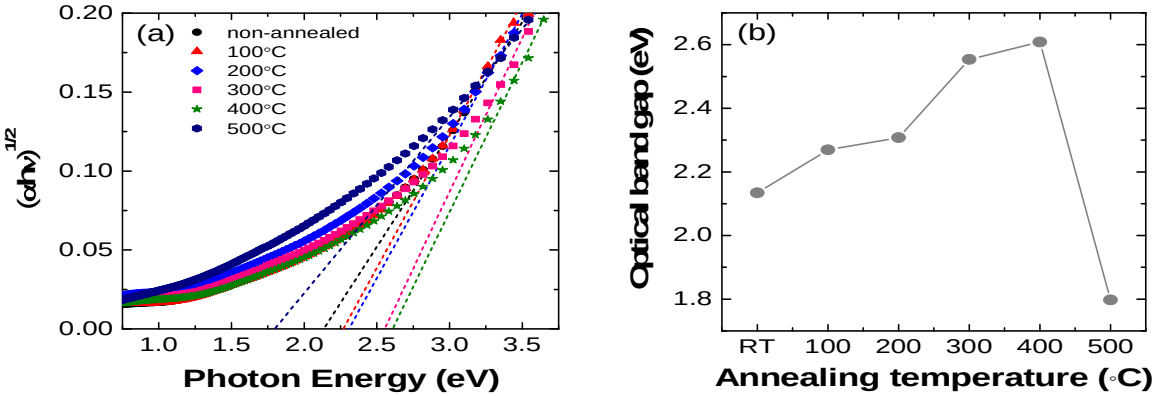

Figure 9. (a) Optical band gap estimation by extrapolation technique, and (b) optical band gap as a function of annealing temperature.

Finally, to verify the phase transformation and the crystallinity of the films in this study, the XRD analysis was carried out as shown in Figure 10. For the acid treated film without annealing, the orthorhombic phase of the $WO_3 \cdot H_2O$ was clearly visible. This confirmed the existence of the water molecules from the acid treatment process. As the annealing temperature increased above 200°C, the phase was transformed to monoclinic phase of the WO_3 film. The residual water molecules were completely eliminated. The crystallinity of the WO_3 was also promoted with higher annealing temperature as observed from the higher monoclinic peak intensities.

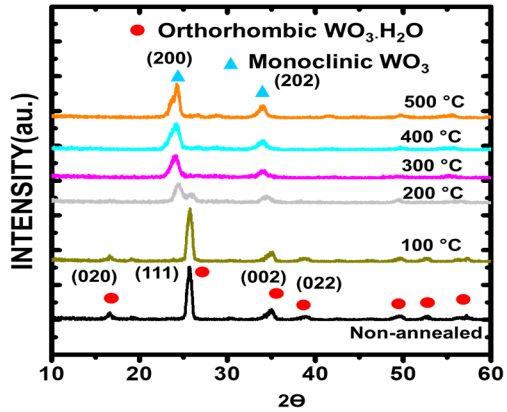

Figure 10. XRD patterns of the $WO_3 \cdot H_2O$ film and WO_3 films with different annealing temperature.

Conclusions

In this research, the WO_3 films with the nanoplate structure were successfully fabricated by the sputtering technique following by acid treatment and annealing. It was found that the $WO_3 \cdot H_2O$ nanostructure film was best formed at the HNO_3 immersion time of 90 min. The $WO_3 \cdot H_2O$ nanostructure film was transformed into the WO_3 film by annealing at temperature of $\geq$ 200°C. The film thickness was decreased as the annealing temperature was higher. The visible optical transmittance increased with the annealing temperature up to 400°C.

Acknowledgements

This work is supported by the Thailand Research Fund (TRF) in cooperation with Khon Kaen University (RSA5980014), and the Nanotechnology Center (NANOTEC), NSTDA, Ministry of Science and Technology, Thailand, through its program of Center of Excellence Network.

References

1. Bignozzi, C.A., et al. (2013). Nanostructured photoelectrodes based on WO_3: applications to photooxidation of aqueous electrolytes. *Chem Soc Rev*. **42(6)**: 2228-46.

2. Horprathum, M., et al. (2013). NO_2-sensing properties of WO_3 nanorods prepared by glancing angle DC magnetron sputtering. *Sensor Actuat B-Chem*. **176**: 685-91.

3. Santato, C., et al. (2001). Crystallographically oriented Mesoporous WO_3 films: Synthesis, characterization, and applications. *J Am Chem Soc*. **123(43)**: 10639-49.

4. Garg, D., et al. (2005). An economic analysis of the deposition of electrochromic WO_3 via sputtering or plasma enhanced chemical vapor deposition. *Mat Sci Eng B-Solid*. **119(3)**: 224-31.

5. Joraid, A.A. (2009). Comparison of electrochromic amorphous and crystalline electron beam deposited WO_3 thin films. *Curr Appl Phys*. **9(1)**: 73-9.

6. Patil, P.S., et al. (2005). Electrochromic properties of spray deposited TiO_2-doped WO_3 thin films. *Appl Surf Sci*. **250(1-4)**: 117-23.

7. Ng, C.Y., et al. (2015). Effect of annealing on acid-treated WO_3 center dot H_2O nanoplates and their electrochromic properties. *Electrochimica Acta*. **178**: 673-81.

8. Li, W.Z., et al. (2012). Platelike WO_3 from hydrothermal RF sputtered tungsten thin films for photoelectrochemical water oxidation. *Materials Letters*. **84**: 41-3.

9. Widenkvist, E., et al. (2008). Synthesis of nanostructured tungsten oxide thin films. *Cryst Growth Des*. **8(10)**: 3750-3.

10. Amano, F., et al. (2011). Facile Preparation of Platelike Tungsten Oxide Thin Film Electrodes with High Photoelectrode Activity. *Acs Appl Mater Inter*. **3(10)**: 4047-52.